

# The role of attraction in the phase diagrams and melting scenarios of generalized 2D Lennard-Jones systems

Elena N. Tsiok,<sup>1</sup> Yuri D. Fomin,<sup>1,2</sup> Evgenii A. Gaiduk,<sup>1</sup> Elena E. Tareyeva,<sup>1</sup> Valentin N. Ryzhov,<sup>1, a)</sup> Pavel A. Libet,<sup>1,3</sup> Nikita A. Dmitryuk,<sup>3</sup> Nikita P. Kryuchkov,<sup>3</sup> and Stanislav O. Yurchenko<sup>3, b)</sup>

<sup>1)</sup>*Institute of High Pressure Physics RAS, 108840 Kaluzhskoe shosse, 14, Troitsk, Moscow, Russia*

<sup>2)</sup>*Moscow Institute of Physics and Technology (National Research University), 9 Institutskiy Lane, Dolgoprudny, Moscow region, 141701, Russia*

<sup>3)</sup>*Bauman Moscow State Technical University, 2nd Baumanskaya street 5, 105005 Moscow, Russia*

(Dated: 6 October 2021)

Monolayer and two-dimensional (2D) systems exhibit rich phase behavior, compared with 3D systems, in particular, due to the hexatic phase playing a central role in melting scenarios. The attraction range is known to affect critical gas-liquid behavior (liquid-liquid in protein and colloidal systems), but the effect of attraction on melting in 2D systems remains unstudied systematically. Here, we reveal how the attraction range affects the phase diagrams and melting scenarios in a 2D system. Using molecular dynamics simulations we considered the generalized Lennard-Jones system with a fixed repulsion branch and different power indices of attraction, from long-range dipolar to short-range sticky-spheres-like. A drop in the attraction range has been found to reduce the temperature of the gas-liquid critical point, bringing it closer to the gas-liquid-solid triple point. At high-temperatures, attraction does not affect the melting scenario that proceeds through the cascade of solid-hexatic (Berezinski-Kosterlitz-Thouless) and hexatic-liquid (first-order) phase transitions. In the case of dipolar attraction, we observed *two triple points*, inherent in a 2D system: hexatic-liquid-gas and crystal-hexatic-gas, the temperature of the crystal-hexatic-gas triple point is *below* the hexatic-liquid-gas triple point. This observation may have far-reaching consequences for future studies, since phase diagrams determine possible routes of self-assembly in molecular, protein, and colloidal systems, whereas the attraction range can be adjusted with complex solvents and external electric or magnetic fields. The results obtained may be widely used in condensed matter, chemical physics, materials science, and soft matter.

## I. INTRODUCTION

Understanding phase transitions in 2D systems has prominent importance in a number of areas, from photonics and electronics, to novel materials and biotechnologies, since the knowledge on phase behavior opens a way to design systems with desired properties. Despite many studies, the fundamental questions here are still related to the effect of particular interaction between individual particles on their collective behavior. For classical systems, one of the simplest models capable of reproducing their behavior, including gas, liquid, and solid phases, is the Lennard-Jones (LJ) system. The LJ model is widely used for analysis of behavior in molecular, protein, polymer, emulsion, and colloidal soft matter<sup>1</sup>. The generalized LJ potential (or the LJn-m-potential, where indices  $n$  and  $m$  are responsible for the algebraic branches of repulsion and attraction, see below) is a suitable model for studies, aimed to reveal the effects of repulsion and attraction on liquids and solids, and the phase transitions between them.

Today, it has been established that 2D melting scenarios depend on *repulsion softness*, providing

the following microscopic scenarios of 2D melting<sup>2,3</sup>: (i) the Berezinskii-Kosterlitz-Thouless-Halperin-Nelson-Young (BKTHNY) theory, according to which melting occurs via two continuous transitions with an intermediary hexatic phase with quasi-long-range orientational order and short-range translational order<sup>4-8</sup>; (ii) melting through a first order phase transition<sup>9,10</sup>; (iii) two-step melting, including a continuous (Berezinskii-Kosterlitz-Thouless, BKT) crystal-hexatic phase transition and a first-order phase transition between the hexatic phase and isotropic liquid<sup>11-15</sup>. The second and third scenarios are inherent in hard-sphere-like systems, whereas the first one was observed for soft repulsion between particles<sup>16-18</sup>. It has been established unambiguously that the softness of repulsion affects melting scenarios, thermodynamics and excitation spectra in monolayer systems<sup>19-32</sup>. However, to the best of our knowledge, the role of *attraction* in the melting scenario of monolayer systems remains unstudied systematically.

LJ interactions were among the first systems studied to understand the role of attraction in melting. However, a lot of reported results on the critical point and melting scenario for 2D LJ crystals still remain questionable. For instance, to provide critical temperature depending on the truncation radius, numerical simulations of a vapor-liquid curve performed in the Gibbs ensemble were reported in Ref.<sup>33</sup>. For critical temperature and density, the authors obtained  $T_c = 0.515 \pm 0.002$  and

<sup>a)</sup>Electronic mail: ryzhov@hppi.troitsk.ru

<sup>b)</sup>Electronic mail: st.yurchenko@mail.ru

$\rho_c = 0.355 \pm 0.003$ , respectively, for the full potential; and  $T_c = 0.459 \pm 0.001$  and  $\rho_c = 0.35 \pm 0.01$  for the truncated and shifted potential at  $2.5\sigma$ . Contradictory melting scenarios of the triangular crystal were reported in the early works<sup>34–39</sup>, including two continuous transitions with an intermediate hexatic phase according to the BKTHNY theory<sup>34</sup> and a first-order transition<sup>35–39</sup>.

Thanks to growth of computing capabilities, simulations of large systems ( $\gtrsim 10^5$  particles) have recently provided new results on 2D melting of LJ crystals and related systems. Simulations of the systems followed by analysis of their equation of state and long-range asymptotics of the translational correlation function (that accurately provides the stability limit of the crystal) allowed identifying the melting scenarios unambiguously. For instance, a change in the melting scenario was reported in Ref.<sup>40</sup>, where the authors studied 2D systems of particles interacting via generalized LJ potential with different repulsive branches ( $\propto 1/r^{12}$  and  $\propto 1/r^{64}$ ). The scenario was found to occur through first-order phase transitions at low temperatures and via two continuous BKT transitions (according to the BKTHNY theory) at high. An LJ system at high temperatures is typically assumed to be close to soft repulsive disks  $1/r^{12}$ , but such extrapolation to a melting scenario contradicts the results of Ref.<sup>14</sup>, wherein the soft disks  $1/r^n$  with  $n > 6$  were shown to melt according to the third melting scenario. The Mayer-Wood loop, inherent in first-order transition, is assumed to disappear at high temperatures with an increase in the system size. However, the explanation of the effect by finite-size scaling seems unconvincing: With an increase in the system size, the loop should flatten and ultimately approach the plateau<sup>12,41</sup>.

A first-order hexatic-liquid transition and a continuous crystal-hexatic BKT transition at high temperatures and one first-order crystal-liquid transition at low temperatures were identified in Ref.<sup>42</sup> for 2D LJ particles. The results of numerical simulation of a 2D LJ system and attractive polygons (squares, pentagons and hexagons) of the same authors in Ref.<sup>43</sup> revealed the role of attraction in a melting scenario. Thus, at low temperatures where the role of attraction is dominant all systems melt via first-order transition due to suppression of the hexatic phase. At high temperatures LJ disks melt in accordance with the third scenario, the same as soft disks<sup>14,44,45</sup>, whereas hexagons and squares do according to the BKTHNY theory with participation of the hexatic and tetratic phases, respectively. The melting scenario of pentagons does not change with an increase in temperature and is a first-order transition.

LJ crystals compared with the Morse system in Ref.<sup>46</sup> were shown to melt via the third scenario at low temperatures and two continuous BKT transitions at high. This agrees with Ref.<sup>40</sup>, but contradicts Refs.<sup>14,42</sup>. The BKTHNY scenario at high temperatures was questioned because of seeming disappearance of the Mayer-Wood loop (an analog of the Van-der-Waals loop in the 3D case). For soft Morse interactions, the third melting scenario

was observed for all temperatures considered in Ref.<sup>46</sup>, whereas the authors expected to observe the BKTHNY scenario at higher temperatures. However, at some parameters of potential softness, two continuous transitions were observed already at low temperatures in the presence of long-range attraction.

The role of attraction can be tested experimentally in colloidal systems, known for a long time as model systems demonstrating a wide range of “molecular-like” phenomena<sup>1,47–50</sup>, in particular, crystallization and melting<sup>51–59</sup>, solid-solid phase transitions<sup>60–62</sup>, condensation and critical phenomena<sup>63–65</sup> caused by relatively *short-range* attractive depletion forces<sup>66</sup>. These collective phenomena can be visualized *in real-time* with spatial resolution of individual particles. *Long-range* dipolar attraction  $\propto 1/r^3$  in colloidal systems can be induced and controlled *in situ* with in-plane rotating magnetic<sup>67–71</sup> or electric<sup>72–79</sup> fields. Using conically-rotating magnetic or electric fields with magic angles, *Van-der-Waals-like attraction* can be created  $\propto 1/r^6$  with “magic” fields<sup>80–83</sup>. Recently, tunable interactions have been achieved by using spatial hodographs of an external electric or magnetic field<sup>84</sup>, by engineering the internal structure<sup>85</sup> and geometry<sup>86</sup> of colloidal particles.

In the present paper, we studied the role of the attraction range in the phase behavior and melting scenarios of a 2D system. Using MD simulations, we considered a generalized Lennard-Jones system with a fixed repulsion branch and different attraction, from long-range dipolar attraction to short-range sticky-spheres-like. A decrease in the attraction range is found to suppress the temperature of the gas-liquid (liquid-liquid in the case of colloid and protein systems) critical point. We found that attraction does not affect melting at high temperatures, occurring through the cascade of solid-hexatic (BKT) and hexatic-liquid (first-order) phase transitions. Surprisingly, at moderate temperatures we observed *two triple points*, hexatic-liquid-gas and crystal-hexatic-gas. The crystal-hexatic-gas triple point for the case of isotropic dipolar attraction has been discovered to be *below* the hexatic-liquid-gas triple point.

## II. SYSTEM AND METHODS

### A. MD details

We studied a system of particles interacting via the generalized Lennard-Jones potential (LJn-m):

$$U_{nm}(r) = \frac{\epsilon}{n-m} \left[ m \left( \frac{\sigma}{r} \right)^n - n \left( \frac{\sigma}{r} \right)^m \right], \quad (1)$$

where  $n$  and  $m$  are the indices of repulsive and attractive branches, respectively, and  $\sigma$  and  $\epsilon$  are the characteristic length of interaction and the depth of the potential well. The potential (1) has minimum  $-\epsilon$  at  $r/\sigma = 1$ . In what follows, we normalized the distances and energies to  $\sigma$

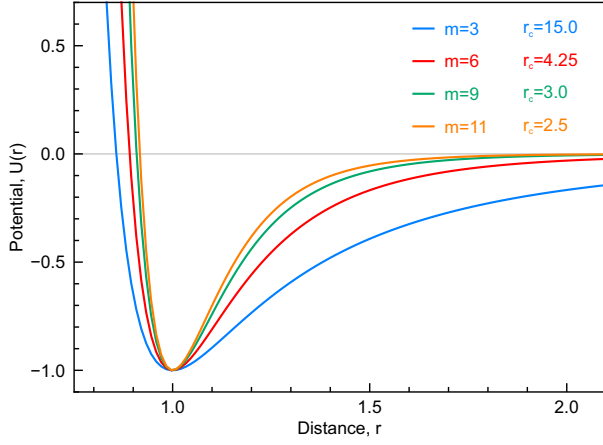


FIG. 1. **Generalised LJ potentials with different attraction indices:** The solid lines correspond to fixed repulsion with  $n = 12$  and different indices  $m = 3, 6, 9$ , and  $11$ , illustrating the transition from long- to short-range attractive interactions. The values of cutoff radii  $r_c$  (used for calculations of the equation of state) decrease as shown for each  $m$ .

and  $\epsilon$ , respectively, and considered the particles of equal mass  $m = 1$ .

We considered cases with fixed repulsion branch  $n = 12$  and different attraction, from long-range isotropic dipolar attraction with  $m = 3$  to short-range almost sticky-spheres-like attraction with  $m = 11$ . Examples of the potentials with  $m = 3, 6, 9$ , and  $11$  are given in Fig. 1. A case similar to usual LJ interaction corresponds to  $n = 12$  and  $m = 6$ .

The molecular dynamics (MD) simulations were performed for  $N = 2 \times 10^4$  particles using LAMMPS in the canonical ( $NVT$ ) ensemble in a wide range of densities and temperatures, from  $T = 0.3$  to  $T = 50.0$ , using  $10^8$  steps with time step  $dt = 10^{-3}$  (in dimensionless units of time normalized to  $\sqrt{m\sigma^2/\epsilon}$ ). The value of potential energy within cutoff radius  $r_c$  was  $|U(r_c)| < 5 \times 10^{-4}$ : it was  $U(r_c) = -4 \times 10^{-4}$  for  $m = 3$ ,  $U(r_c) = -3.4 \times 10^{-4}$  for  $m = 6$ ,  $U(r_c) = -2 \times 10^{-4}$  for  $m = 9$ ,  $U(r_c) = -3.2 \times 10^{-4}$  for  $m = 11$ . To determine accurately the boundaries of two-phase areas,

crystal melting was examined (at some points) for large systems with  $N = 256^2$  and  $512^2$  particles. The phase diagram was obtained using the dependence of pressure on density (the equation of state) along the isotherms, analysis of the radial distribution functions, orientational and translational order parameters, and the corresponding correlation functions.

## B. The method of phase identification

The condensate-gas binodals were obtained using the method of phase identification, proposed in Ref.<sup>87</sup>. The method allows obtaining a binodal in the coordinates density-temperature using analysis of Voronoi cells in the system and, in particular, in terms of the following order parameter<sup>59,87</sup>:

$$\lambda_i = \frac{1}{N_{ni} + 1} \left( \sigma_i + \sum_{j=1}^{N_{ni}} \sigma_j \right), \quad (2)$$

$$\sigma_i = \frac{1}{a_i N_{ni}} \sqrt{\sum_{j < k}^{N_{ni}} (r_{ij} - r_{ik})^2 / 2}, \quad r_{ij} = |\mathbf{r}_i - \mathbf{r}_j|,$$

where  $\mathbf{r}_i$  is the radius-vector of the  $i$ -th particle,  $N_{ni}$  is the number of its neighboring cells,  $a_i = \sqrt{S_i/\pi}$ ,  $S$  is the area of a corresponding Voronoi cell. The scalar  $\lambda^2$ -field has small values for condensed (liquid and solid) phases, and becomes large at the interface gas-condensate and in gaseous state. Then, analysis of corresponding statistics of Voronoi cells allows obtaining densities  $n_c$  and  $n_g$  of condensate and gas, respectively (see Ref.<sup>87</sup> for details).

To apply the method, additional simulations of a small system with  $N = 3.6 \times 10^3$  particles under the same  $NVT$  conditions (as we explained above), from  $T_{start}$  to  $T_{stop}$ , with step  $T_{step}$  were conducted where each step included  $6 \times 10^5$  time-steps with dimensionless time-step  $\Delta t = 5 \times 10^{-4}$  (see the parameters in Table I). At each temperature, we performed phase identification using  $10^2$  simulation frames.

This method of phase identification becomes unsuitable near the critical point, where the condensed and

TABLE I. **Simulation parameters for potentials LJ12-m used for calculations in the phase identification method, where  $a = \rho^{-1/2}$**

LJn-m	$\rho$	$r_c$	$T_{start}$	$T_{stop}$	$T_{step}$
LJ12-3	0.3	7.5a	0.7	3.05	0.06
LJ12-4	0.4	7.5a	0.1	2.0	0.03
LJ12-5	0.4	7.5a	0.1	1.5	0.02
LJ12-6	0.4	7.5a	0.1	1.5	0.02
LJ12-7	0.4	7.5a	0.454	0.503	0.003
LJ12-8	0.4	7.5a	0.2	0.4	0.003
LJ12-9	0.4	7.5a	0.14	0.3	0.002
LJ12-10	0.4	5.0a	0.09	0.151	0.001
LJ12-11	0.5	5.0a	0.025	0.076	0.001

TABLE II. **The temperatures and densities in the critical and triple points obtained using the phase identification method**

LJn-m	$T_{CP}$	$\rho_{CP}$	$T_{TP}$	$\rho_{TP}$
LJ12-3	1.442	0.366	0.577	1.095
LJ12-4	0.748	0.453	0.455	1.042
LJ12-5	0.606	0.466	0.408	1.017
LJ12-6	0.510	0.488	0.390	1.012
LJ12-7	0.480	0.486	0.399	1.015
LJ12-8	0.436	0.509	0.390	1.016
LJ12-9	0.429	0.516	0.393	1.029
LJ12-10	0.410	0.544	0.386	0.996
LJ12-11	0.4053	0.550	0.3844	1.0478

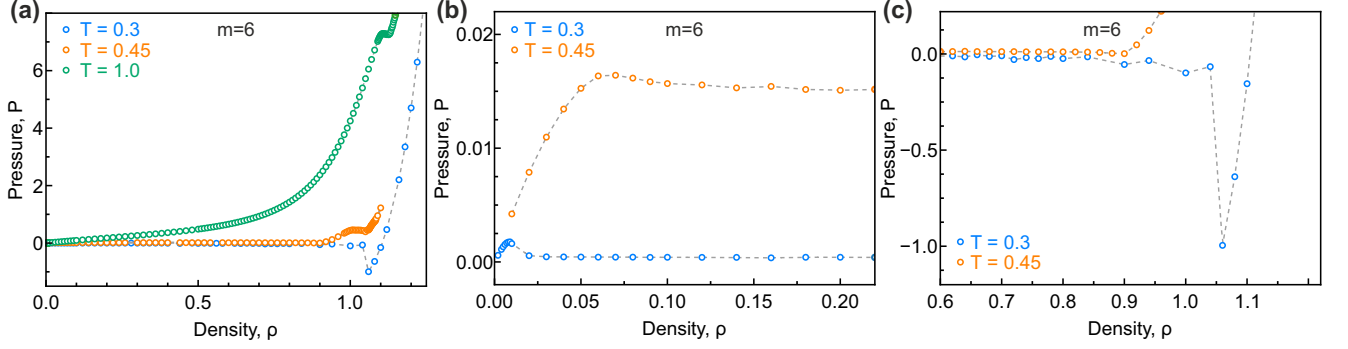


FIG. 2. **The equation of state for the 2D LJ system:** (a) The isotherms of the system with  $m = 6$  below ( $T = 0.3$ ) and above ( $T = 0.45$ ) the triple point and above the critical point at  $T = 1.0$ . (b) Isotherm  $T = 0.45$  gas-liquid and isotherm  $T = 0.3$  gas-crystal at low densities. (c) Isotherm  $T = 0.45$  gas-liquid and isotherm  $T = 0.3$  gas-crystal at high densities.

gaseous phases cannot be distinguished. However, one can obtain the values of critical density  $n_{CP}$  and temperature  $T_{CP}$  using the following approximation of the binodal (the results are provided in Table II):

$$n_c - n_g \simeq A\tau^\beta, \quad n_c + n_g \simeq a\tau + 2n_{CP}, \quad (3)$$

where  $\tau = T_{CP} - T$  is reduced temperature,  $\beta$  is a critical index,  $A$  and  $a$  are the free parameters of the model. Critical index  $\beta$  is related to the universality class of the system and is determined by the range of attraction<sup>88</sup>: In 2D systems with dipolar isotropic attraction,  $\beta = 1/2$  (mean-field critical behavior), whereas in the case of shorter-range attraction, at  $m > 3$ ,  $\beta = 1/8$  corresponds to 2D Ising behavior<sup>88</sup>.

### C. Order parameters

For analysis of the phase transition scenarios, we used orientational and translational correlation functions. The orientational correlation function (OCF) of the global orientational order parameter is calculated as:

$$G_6(r) = \frac{\langle \Psi_6(\mathbf{r}) \Psi_6^*(0) \rangle}{g(r)}, \quad \Psi_6 = \frac{1}{N} \left\langle \left| \sum_i \psi_6(\mathbf{r}_i) \right| \right\rangle, \quad (4)$$

where the averaging for  $G_6$  is performed over all particles in the system,  $\psi_6 = 1/n(i) \sum_j e^{6i\theta_{ij}}$ ,  $\theta_{ij}$  is the angle of the vector between particles  $i$  and  $j$  with respect to the reference axis, and the sum over  $j$  is counting the  $n(i)$  nearest-neighbors of  $j$ , obtained from the Voronoi construction,  $g(r) = \langle \delta(\mathbf{r}_i) \delta(\mathbf{r}_j) \rangle$  is an isotropic pair distribution function (here,  $\mathbf{r}_i$  is the position vector of particle  $i$ , and  $r = |\mathbf{r}_i - \mathbf{r}_j|$ ). In the hexatic phase,  $G_6(r)$  behaves at large distances like  $G_6(r) \propto r^{-\eta_6}$  with  $\eta_6 \leq 1/4$ <sup>6,7</sup>.

The translational correlation function (TCF) is

$$G_t(r) = \frac{\langle \exp(i\mathbf{a}(\mathbf{r}_i - \mathbf{r}_j)) \rangle}{g(r)}, \quad (5)$$

where  $\mathbf{a}$  is the reciprocal-lattice vector of the first shell of the crystal lattice. In the solid phase,  $G_t(r)$  behaves

at large distances like  $G_t(r) \propto r^{-\eta_T}$  with  $\eta_T \leq 1/3$ <sup>6,7</sup>. In the hexatic phase and isotropic liquid,  $G_t$  decays exponentially.

## III. RESULTS AND DISCUSSION

### A. The equations of state and phase diagrams

The equations of state (isotherms) for all considered systems behave in a similar manner and have peculiarities that, depending on the temperature and density, attributed to gas-liquid transition or crystal melting, respectively. This is shown in Fig. 2(a): Here, at isotherm  $T = 0.45$ , one can see a wide loop peculiar to gas-liquid transition and a narrow loop related to crystal melting, whereas only one loop related to crystal melting is seen above the gas-liquid critical point at  $T = 1.0$ . Below the triple point, at  $T = 0.3$ , there is only one wide loop corresponding to gas-crystal transition.

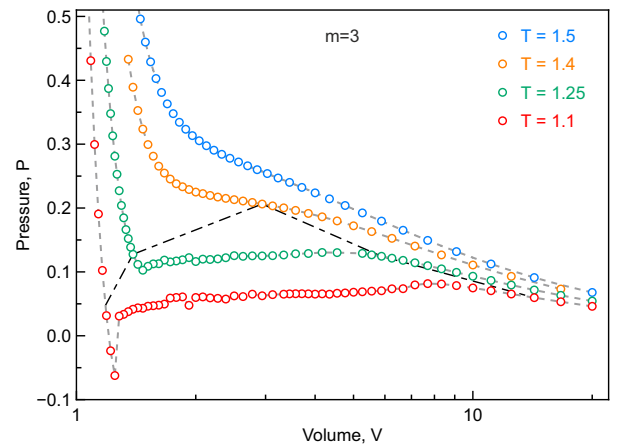


FIG. 3. **The isotherms of LJ12-3 system in  $P-V$  coordinates:** The gas-liquid transition boundary is obtained using Maxwell's construction at different temperatures and is shown with the black dashdotted line.

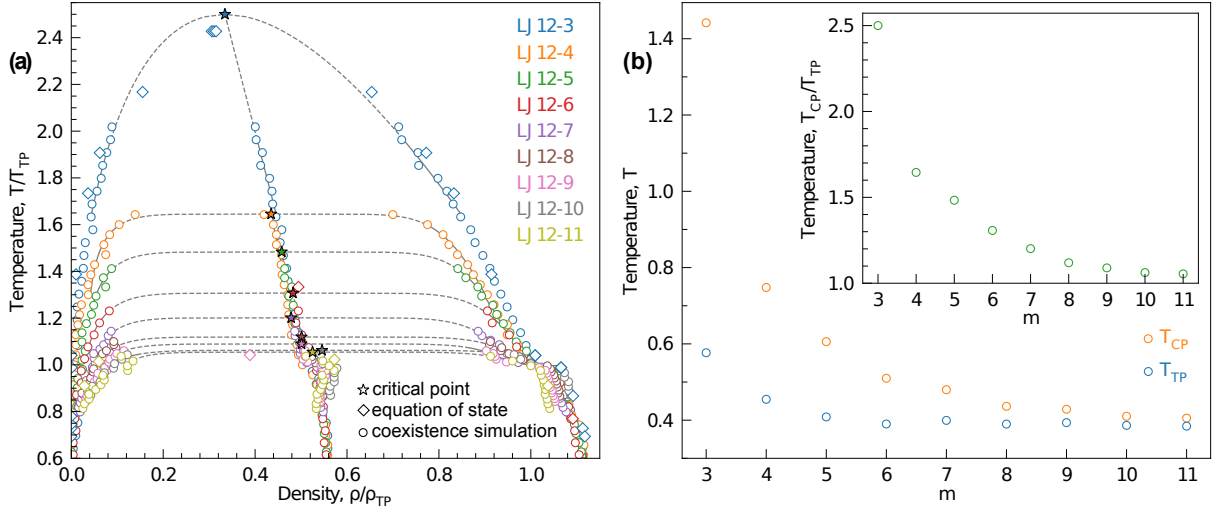


FIG. 4. **The effect of the attraction range on the liquid-gas coexistence area on the phase diagram:** (a) The binodals condensate-gas for different LJ12- $m$  potentials; the circles are the points of the binodal and median (obtained using the phase identification method), the diamonds are points obtained from the equation of state, the grey lines are the approximations of the binodal with Eq. (3), the stars denote the critical points from Table II. (b) The dependencies of triple and critical temperatures on attraction index  $m$  for LJ12- $m$  interaction, the ratio  $T_{CP}/T_{TP}$  is shown in the inset.

The binodals gas-liquid were calculated using Maxwell's construction on the isotherms in the  $P - V$  coordinates (an example is shown in Fig. 3 for the system with  $m = 3$ ), as well as with the phase identification method. The results for the binodal condensate-gas obtained from the phase identification method and the equation of state are provided in Fig. 4(a). Here, the colored circles denote the densities of gas, condensate, and their average for each potential we considered. The grey solid lines show the regions of the data wherein we used the approximation (3) to obtain data about the critical point. The grey dashed lines show the extrapolation of the phase diagram to the critical points gas-liquid, depicted with colored stars (the corresponding densities and temperatures are given in Table II).

We observed that the drop in the attraction range reduces the critical temperature, as well as the ratio between temperatures of the critical and triple points, as shown in Fig. 4(b) and the corresponding inset (based on the data in Table II). With an increase in  $m$  (short-range attraction), the two-phase area becomes narrower towards lower densities and the ratio between the critical and triple temperatures becomes closer to unity, as shown in Fig. 4(b). For LJ interaction ( $m = 6$ ), the critical temperature we obtained is  $T_c = (0.51 \dots 0.52)$  (depending on the method of evaluation), which agrees well with the previous results  $T_c = 0.515 \pm 0.002$  for the LJ potential reported in Ref.<sup>33</sup>.

At high temperatures, the effect of attraction should vanish, and only the repulsive branch of potential (1) should play a more significant role. Indeed, analyzing the melting scenarios of triangular crystals at high temperatures (and high densities), we observed that LJ12- $m$  systems demonstrated the same melting scenarios as

soft disks repulsive potential  $1/r^{12}$  (the third melting scenario<sup>14,42,45</sup>).

The Mayer-Wood loop was observed in all considered systems at high temperatures, proving first-order transition. However, to determine an appropriate melting scenario, we compared the stability limits of the crystal and the hexatic phases with the boundaries of the Mayer-Wood loop. The stability limits of the hexatic and crystal phases were derived from asymptotic behavior of the correlation functions of the orientational and translational order parameters, respectively. An example of evolution of the correlation functions on the isotherm of the LJ system at  $T = 3.0$  is shown in Fig. 5.

In Fig. 5(a), the equation of state is shown at  $T = 3.0$  (obtained by averaging over 20 independent replicas) for the LJ system consisting of  $N = 512^2$  particles. One can see the clearly defined Mayer-Wood loop, inherent in first-order transitions. Analyzing the correlation functions in Figs. 5(b,c), we conclude that the loop corresponds to the two-phase hexatic-liquid area, whereas the melting scenario is the third, with a continuous BKT transition from crystal to hexatic and a first-order transition from hexatic to liquid. Here, the hexatic phase becomes unstable at  $\rho_{hex-liq} = 1.014$  (Fig. 5(b)), inside the loop, whereas the crystal becomes unstable at  $\rho_{sol-hex} = 1.037$  (Fig. 5(c)) getting far out of the loop. The obtained results agree well with the melting scenario for repulsive disks  $1/r^{12}$  (reported in Refs.<sup>14,42,45</sup>), but do not exhibit two continuous BKT transitions in the LJ system at high temperatures<sup>12,89</sup>. The obtained results agree well with the melting scenario for repulsive disks  $1/r^{12}$  (reported in Refs.<sup>14,42,45</sup>), but do not exhibit two continuous BKT transitions in the LJ system at high temperatures<sup>12,89</sup>.

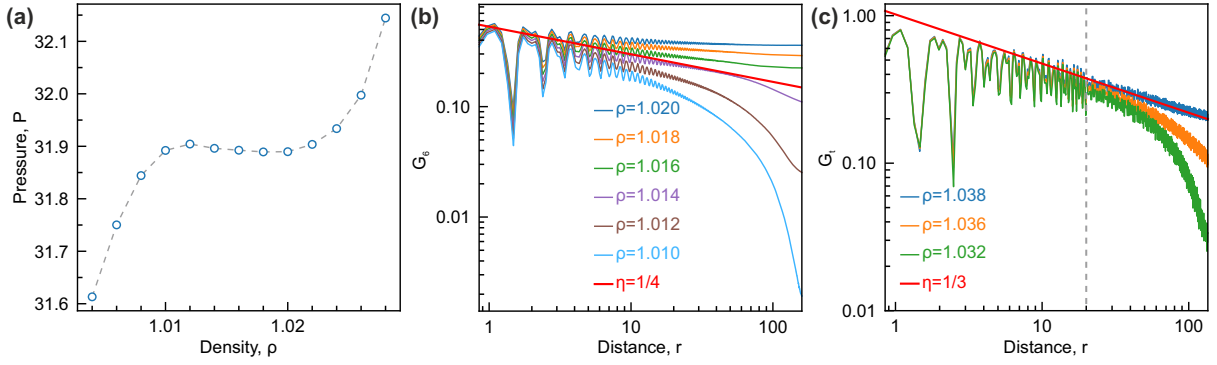


FIG. 5. **Evolution of correlation functions on an isotherm:** (a) The isotherm  $T = 3.0$  for LJ system consisting of  $N = 512^2$ , obtained by averaging over 20 independent replicas. (b) and (c) The OCF and TCF for the same system at different densities.

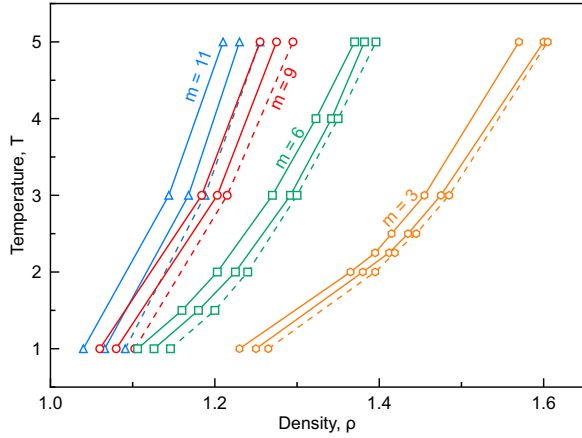


FIG. 6. **The third melting scenario of the triangular crystals at high temperatures and densities:** The solid lines are the boundaries of the Mayer-Wood loop corresponding to the two-phase hexatic-liquid area. The dashed lines are the boundaries of BKT transition from the crystal to hexatic phase. The results are provided for the cases  $m = 3, 6, 9$ , and  $11$ , as labeled in the figure.

All triangular crystals, we studied, were found to melt at high temperatures via the third scenario, irrespective to the attraction index  $m$ . The melting lines in this region of the phase diagram are shifted to low densities with an increase in  $m$  and behave similarly to a system of soft disks  $1/r^{12}$ , as shown in Fig. 6.

However, with a decrease in melting temperature, the balance of the effects provided by the repulsive and attractive branches is changed. As a result, we observed that, at low temperatures, the melting scenario *changes* from the third one to a first-order transition (without inclusion of the hexatic phase) in the systems with  $m = 6, 9$ , and  $11$ . The change in the melting scenario is shown for two isotherms of the LJ12-9 system in Fig. 7.

The temperature of the observed change in the melting scenario decreases with  $m$  (to more soft and long-range attraction). The attraction range affects essentially the

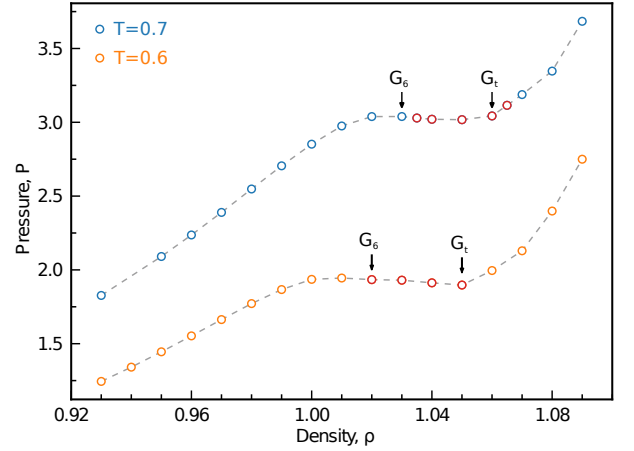


FIG. 7. **The change in the melting scenario for the case  $m = 9$ :** The melting scenario changes from a first-order transition ( $T = 0.6$ ) to the third scenario ( $T = 0.7$ ). The arrows show the stability limits of the hexatic phase,  $G_6$  are obtained using the OCF, and the stability limits of the crystalline phase,  $G_t$  are obtained with TCF, which become caught by the loop with a decrease in temperature.

region of gas-liquid transition, as well as temperatures  $T_c$  and  $T_m$ , at which the hexatic phase appears.

## B. The results for isotropic dipolar attraction

In the case of LJ12-3 potential, the crystal was found to melt at low temperatures according to the third scenario. However, the hexatic phase was discovered to be preserved up to triple point temperature  $T_t$ , where it coexists with both liquid and gaseous phases, as given in Fig. 8.

This unexpected result is explained using the Gibbs rule: Due to the reduced spatial dimension and since melting represents a two-stage process, we obtain a couple of points where three phases may exist simul-



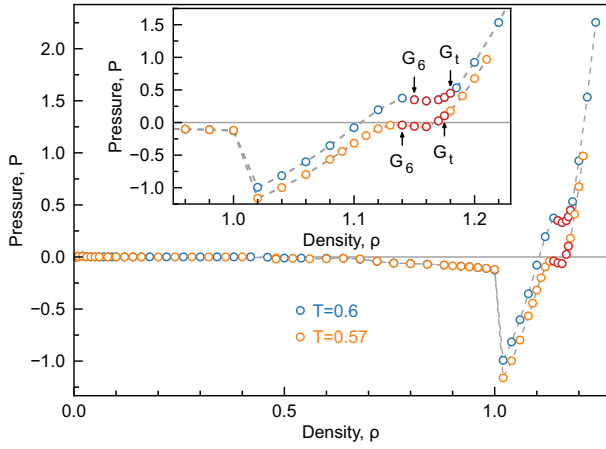


FIG. 8. **The cascades of phase transitions:** Isotherm  $T = 0.6 > T_t$  illustrates the cascade of a first-order gas-liquid transition, first-order liquid-hexatic transition, and a continuous BKT crystal-hexatic transition. At  $T = 0.57 < T_t$ , only a first-order gas-hexatic transition and a continuous BKT crystal-hexatic transition are seen. Detailed behavior of the isotherms at high densities are shown in the inset. At negative pressures and  $T = 0.57 < T_t$ , one can see a loop related to the first-order transition gas-hexatic (in the metastable area), while a continuous BKT crystal-hexatic transition still occurs at positive pressure. The arrows show the limits of stability of the hexatic phase  $G_6$  and of the crystal  $G_t$ , obtained using OCF and TCF analysis, respectively.

taneously: hexatic-liquid-gas (at temperature  $T_{t1}$ ) and crystal-hexatic-gas (at lower temperature  $T_{t2} < T_{t1}$ ). This situation is caused by appearance of an additional (hexatic) phase, inherent in 2D systems, and stands in contrast to simple bulk systems, where only one triple point gas-liquid-solid may exist. In the interval  $T_{t2} < T_{t1}$ , a continuous BKT transition from the crystal to hexatic phase and a first-order transition from hexatic to gas occur up to the crystal-gas sublimation line, at which a first-order transition from crystal to gas is observed on the isotherms. Simulation of first-order gas-solid transitions at temperatures below  $T_{t2}$  for finite systems inevitably leads to the appearance of metastable states. This is manifested by the Mayer-Wood loops, strongly extended due to a large difference of densities on the isotherms. Moreover, these loops turn out to have a complex structure, as given in Fig. 9.

At high densities in the vicinity of the crystalline phase, additional modulations of the loops may be interpreted as two-stage melting of the metastable crystal appearing in the equation of state. In this case, phase identification was performed using analysis of the radial distribution functions, behavior of the orientational and translational order parameters, and their correlation functions. We observed a transition of the metastable crystal to the hexatic phase through a continuous BKT transition with a subsequent first-order transition from hexatic to gas. With a decrease in temperature, the region of the hexatic phase narrows on the phase diagram,

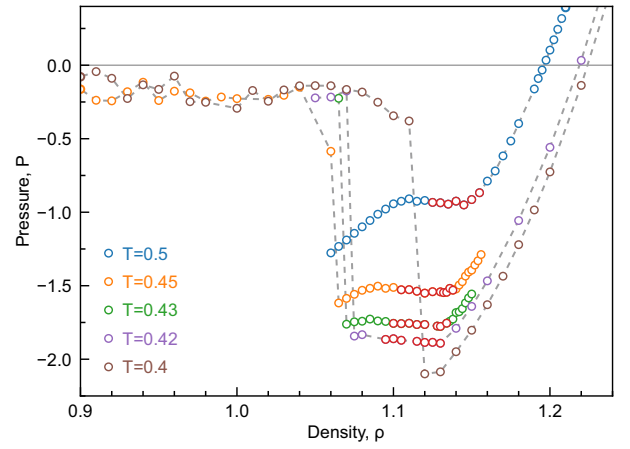


FIG. 9. The isotherms of the LJ system at temperatures  $T < T_{t2}$  in the high-density region.

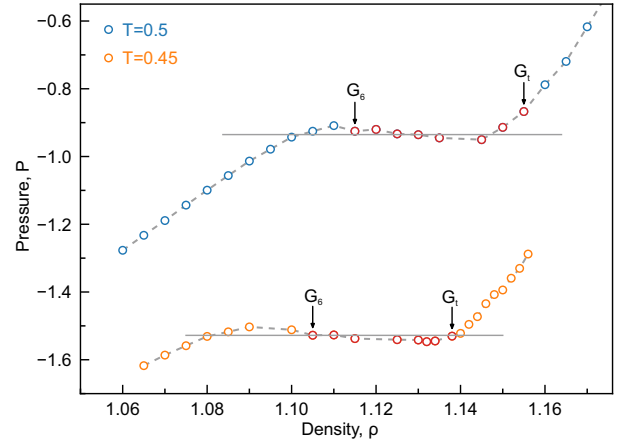


FIG. 10. The change of the transition scenario from the third scenario (isotherm  $T = 0.5$ ) to a first-order transition (isotherm  $T = 0.45$ ) in the area of negative pressures at  $T < T_{t2}$ , which is related to suppression of the hexatic phase at  $T = 0.45$ .

and disappears completely at  $T = 0.45$ , which leads to one first-order crystal-gas transition, as shown in Fig. 10.

For the case of isotropic dipolar attraction  $m = 3$ , the phase diagrams in different coordinates are presented in Figs. 11(a,b). Here, the lines of phase coexistence, critical, and triple points are shown in Fig. 11(a). In the density-temperature plane, a two-stage crystal-gas transition occurs in the metastable area of the hexatic phase and crystal at  $T < T_{t2}$ , see Fig. 11(b). In Fig. 11(c) an enlargement of the phase diagram is represented the behavior of different domain boundaries on the phase diagram near triple points  $T_{t1}$  and  $T_{t2}$ . We note in conclusion that, with an increase in the number of particles in the system, the loops corresponding to gas-crystal transition should flatten. This leads to the disappearance of the metastable area of the crystal and to the first-order gas-crystal transition, without the modulation of

the equation of state mentioned above.

#### IV. CONCLUSIONS

In this work, we studied the evolution of the phase diagrams and melting scenarios of two dimensional systems of particles interacting via generalized LJ potential with a different attraction range, whereas the repulsion branch was fixed. Gas-liquid transition was studied using analysis of the equation of state and the phase identification method. The results obtained by the two methods stand in good agreement indicating their consistency. The drop in the attraction range reduces the gas-liquid coexistence region and temperatures of the critical and triple points.

Melting at high temperatures (and high densities) is found to behave like a system of soft disks  $1/r^{12}$ , via the third scenario. However, at low melting temperatures, a change in the melting scenario was identified from the third scenario to a first-order transition (without the hexatic phase) in the systems with  $m = 6, 9$ , and  $11$ . The temperature of the change in the scenarios is shifted toward lower temperatures with an increase in the attraction range (corresponding to the decrease in  $m$ ). Analysis of the case  $m = 9$  (LJ12-9), very close to that studied in Ref.<sup>65</sup>, demonstrated that for short-range attraction in complex solvents we should witness the third melting scenario.

The largest region of gas-liquid coexistence was observed in the phase diagram in the  $\rho - T$  coordinates in the case of  $m = 3$ . Due to soft long-range isotropic dipolar attraction, we unexpectedly saw two triple points at  $T_{t1}$  and  $T_{t2}$ , corresponding to hexatic-liquid-gas and to crystal-hexatic-gas equilibrium, respectively. On the isotherms in the interval between two triple points  $T_{t2}$  and  $T_{t1}$ , we observed a continuous BKT transition from crystal to hexatic phase and a first-order transition from hexatic to gas. At the crystal-gas sublimation line, a first-order transition from crystal to gas has been identified.

The main conclusions related to the scenario of phase transitions in a system with dipolar attraction can be tested in future experiments with colloidal systems, wherein the tunable long-range dipolar attraction can be created with rotating magnetic or electric fields. A nontrivial question here is related to the role of three-body forces, inherent in atomic materials and tunable colloids<sup>78,79</sup>. LJ-like interactions can be created with magic hodographs of rotating electric or magnetic fields<sup>84</sup>. However, three-body interactions in this case behave as  $\propto 1/r^6$ , with the same asymptotics as pairwise potential. Due to this, the scenario of melting can change, and we leave the corresponding study to future work.

#### ACKNOWLEDGMENTS

The study was supported by the Russian Science Foundation, Grant No. 19-12-00092 (MD simulations to obtain phase diagrams) and 20-12-00356 (analysis with phase identification method). This work was carried out using computing resources of the federal collective usage center “Complex for simulation and data processing for mega-science facilities” at NRC “Kurchatov Institute”, <http://ckp.nrcki.ru>, and supercomputers at Joint Supercomputer Center of the Russian Academy of Sciences (JSCC RAS).

E.N.T., Y.D.F., and E.A.G. performed MD simulations to obtain phase diagrams, N.A.D., P.A.L., and N.P.K. obtained condensate-gas binodals with phase identification method, E.N.T., V.N.R., E.E.T., N.P.K., and S.O.Y. analysed and discussed the results, E.N.T., V.N.R., and S.O.Y. wrote the manuscript, V.N.R. and S.O.Y. conceived and directed the study.

- <sup>1</sup>A. Fernandez-Nieves and A. M. Puertas, *Fluids, colloids, and soft materials: an introduction to soft matter physics* (Wiley, 2016).
- <sup>2</sup>V. N. Ryzhov, E. E. Tareyeva, Y. D. Fomin, and E. N. Tsiok, “Berezinskii – kosterlitz – thouless transition and two-dimensional melting,” *Physics-Uspekhi* **60**, 857–885 (2017).
- <sup>3</sup>V. N. Ryzhov, E. E. Tareyeva, Y. D. Fomin, and E. N. Tsiok, “Complex phase diagrams of systems with isotropic potentials: results of computer simulations,” *Physics-Uspekhi* **63**, 417–439 (2020).
- <sup>4</sup>V. L. Berezinsky, “Destruction of long range order in one-dimensional and two-dimensional systems having a continuous symmetry group. i. classical systems,” *Sov. Phys. JETP* **32**, 493–500 (1971).
- <sup>5</sup>J. M. Kosterlitz and D. J. Thouless, “Ordering, metastability and phase transitions in two-dimensional systems,” *Journal of Physics C: Solid State Physics* **6**, 1181–1203 (1973).
- <sup>6</sup>B. I. Halperin and D. R. Nelson, “Theory of two-dimensional melting,” *Physical Review Letters* **41**, 121–124 (1978).
- <sup>7</sup>D. R. Nelson and B. I. Halperin, “Dislocation-mediated melting in two dimensions,” *Physical Review B* **19**, 2457–2484 (1979).
- <sup>8</sup>A. P. Young, “Melting and the vector coulomb gas in two dimensions,” *Physical Review B* **19**, 1855–1866 (1979).
- <sup>9</sup>S. T. Chui, “Grain-boundary theory of melting in two dimensions,” *Physical Review B* **28**, 178–194 (1983).
- <sup>10</sup>V. Ryzhov, “Dislocation-disclination melting of two-dimensional lattices,” *JETP* **73**, 899 (1991).
- <sup>11</sup>E. P. Bernard and W. Krauth, “Two-step melting in two dimensions: First-order liquid-hexatic transition,” *Physical Review Letters* **107**, 155704 (2011).
- <sup>12</sup>M. Engel, J. A. Anderson, S. C. Glotzer, M. Isobe, E. P. Bernard, and W. Krauth, “Hard-disk equation of state: First-order liquid-hexatic transition in two dimensions with three simulation methods,” *Physical Review E* **87**, 042134 (2013).
- <sup>13</sup>W. Qi, A. P. Gantapara, and M. Dijkstra, “Two-stage melting induced by dislocations and grain boundaries in monolayers of hard spheres,” *Soft Matter* **10**, 5449 (2014).
- <sup>14</sup>S. C. Kapfer and W. Krauth, “Two-dimensional melting: From liquid-hexatic coexistence to continuous transitions,” *Physical Review Letters* **114**, 035702 (2015).
- <sup>15</sup>A. L. Thorneywork, J. L. Abbott, D. G. Aarts, and R. P. Dullens, “Two-dimensional melting of colloidal hard spheres,” *Physical Review Letters* **118**, 158001 (2017).
- <sup>16</sup>D. E. Dudalov, E. N. Tsiok, Y. D. Fomin, and V. N. Ryzhov, “Effect of a potential softness on the solid-liquid transition in a



- two-dimensional core-softened potential system,” *The Journal of Chemical Physics* **141** (2014), 10.1063/1.4896825.
- <sup>17</sup>D. E. Dudalov, Y. D. Fomin, E. N. Tsiok, and V. N. Ryzhov, “How dimensionality changes the anomalous behavior and melting scenario of a core-softened potential system?” *Soft Matter* **10**, 4966–4976 (2014).
  - <sup>18</sup>V. Ryzhov and E. Tareyeva, “Melting in two dimensions: first-order versus continuous transition,” *Physica A-Statistical Mechanics and Its Applications* **314**, 396–404 (2002), Meeting on Horizons in Complex Systems, MESSINA, ITALY, DEC, 2001.
  - <sup>19</sup>E. N. Tsiok, D. E. Dudalov, Y. D. Fomin, and V. N. Ryzhov, “Random pinning changes the melting scenario of a two-dimensional core-softened potential system,” *Physical Review E* **92** (2015), 10.1103/PhysRevE.92.032110.
  - <sup>20</sup>L. Pomirchi, V. Ryzhov, and E. Tareyeva, “Melting of two-dimensional systems: Dependence of the type of transition on the radius of the potential,” *Theoretical and Mathematical Physics* **130**, 101–110 (2002).
  - <sup>21</sup>V. V. Brazhkin, A. G. Lyapin, V. N. Ryzhov, K. Trachenko, Y. D. Fomin, and E. N. Tsiok, “Where is the supercritical fluid on the phase diagram?” *Physics-Uspekhi* **55**, 1061–1079 (2012).
  - <sup>22</sup>N. P. Kryuchkov, S. A. Khrapak, and S. O. Yurchenko, “Thermodynamics of two-dimensional yukawa systems across coupling regimes,” *The Journal of Chemical Physics* **146**, 134702 (2017).
  - <sup>23</sup>S. A. Khrapak, N. P. Kryuchkov, and S. O. Yurchenko, “Thermodynamics and dynamics of two-dimensional systems with dipole-like repulsive interactions,” *Physical Review E* **97**, 022616 (2018).
  - <sup>24</sup>N. P. Kryuchkov, E. V. Yakovlev, E. A. Gorbunov, L. Couedel, A. M. Lipaev, and S. O. Yurchenko, “Thermoacoustic instability in two-dimensional fluid complex plasmas,” *Physical Review Letters* **121**, 075003 (2018).
  - <sup>25</sup>N. P. Kryuchkov, L. A. Mistryukova, V. V. Brazhkin, and S. O. Yurchenko, “Excitation spectra in fluids: How to analyze them properly,” *Scientific Reports* **9**, 10483 (2019).
  - <sup>26</sup>N. P. Kryuchkov, V. V. Brazhkin, and S. O. Yurchenko, “Anticrossing of longitudinal and transverse modes in simple fluids,” *The Journal of Physical Chemistry Letters* **10**, 4470–4475 (2019).
  - <sup>27</sup>E. V. Yakovlev, N. P. Kryuchkov, P. V. Ovcharov, A. V. Sapelkin, V. V. Brazhkin, and S. O. Yurchenko, “Direct experimental evidence of longitudinal and transverse mode hybridization and anticrossing in simple model fluids,” *The Journal of Physical Chemistry Letters* **11**, 1370–1376 (2020).
  - <sup>28</sup>N. P. Kryuchkov, L. A. Mistryukova, A. V. Sapelkin, V. V. Brazhkin, and S. O. Yurchenko, “Universal effect of excitation dispersion on the heat capacity and gapped states in fluids,” *Physical Review Letters* **125**, 125501 (2020).
  - <sup>29</sup>S. Khrapak, N. P. Kryuchkov, L. A. Mistryukova, and S. O. Yurchenko, “From soft- to hard-sphere fluids: Crossover evidenced by high-frequency elastic moduli,” *Physical Review E* **103**, 052117 (2021).
  - <sup>30</sup>Y. D. Fomin, E. A. Gaiduk, E. N. Tsiok, and V. N. Ryzhov, “The phase diagram and melting scenarios of two-dimensional Hertzian spheres,” *Molecular Physics* **116**, 3258–3270 (2018).
  - <sup>31</sup>E. N. Tsiok, E. A. Gaiduk, Y. D. Fomin, and V. N. Ryzhov, “Melting scenarios of two-dimensional Hertzian spheres with a single triangular lattice,” *Soft Matter* **16**, 3962–3972 (2020).
  - <sup>32</sup>E. N. Tsiok, Y. D. Fomin, E. A. Gaiduk, and V. N. Ryzhov, “Structural transition in two-dimensional Hertzian spheres in the presence of random pinning,” *Physical Review E* **103** (2021), 10.1103/PhysRevE.103.062612.
  - <sup>33</sup>B. Smit and D. Frenkel, “Vapor–liquid equilibria of the two-dimensional lennard-jones fluid(s),” *The Journal of Chemical Physics* **94**, 5663–5668 (1991).
  - <sup>34</sup>D. Frenkel and J. P. McTague, “Evidence for an orientationally ordered two-dimensional fluid phase from molecular-dynamics calculations,” *Physical Review Letters* **42**, 1632–1635 (1979).
  - <sup>35</sup>S. Toxvaerd, “Melting in a two-dimensional lennard-jones system,” *The Journal of Chemical Physics* **69**, 4750–4752 (1978).
  - <sup>36</sup>F. F. Abraham, “Melting in two dimensions is first order: An isothermal-isobaric monte carlo study,” *Physical Review Letters* **44**, 463–466 (1980).
  - <sup>37</sup>J. M. Phillips, L. W. Bruch, and R. D. Murphy, “The two-dimensional lennard-jones system: Sublimation, vaporization, and melting,” *The Journal of Chemical Physics* **75**, 5097–5109 (1981).
  - <sup>38</sup>A. F. Bakker, C. Bruin, and H. J. Hilhorst, “Orientational order at the two-dimensional melting transition,” *Physical Review Letters* **52**, 449–452 (1984).
  - <sup>39</sup>K. J. Strandburg, J. A. Zollweg, and G. V. Chester, “Bond-angular order in two-dimensional lennard-jones and hard-disk systems,” *Physical Review B* **30**, 2755–2759 (1984).
  - <sup>40</sup>A. Hajibabaei and K. S. Kim, “First-order and continuous melting transitions in two-dimensional lennard-jones systems and repulsive disks,” *Physical Review E* **99**, 022145 (2019).
  - <sup>41</sup>J. J. Alonso and J. F. Fernández, “van der waals loops and the melting transition in two dimensions,” *Physical Review E* **59**, 2659–2663 (1999).
  - <sup>42</sup>Y.-W. Li and M. P. Ciamarra, “Phase behavior of lennard-jones particles in two dimensions,” *Physical Review E* **102**, 062101 (2020).
  - <sup>43</sup>Y.-W. Li and M. P. Ciamarra, “Attraction tames two-dimensional melting: From continuous to discontinuous transitions,” *Physical Review Letters* **124**, 218002 (2020).
  - <sup>44</sup>E. N. Tsiok, Y. D. Fomin, and V. N. Ryzhov, “Random pinning elucidates the nature of melting transition in two-dimensional core-softened potential system,” *Physica A-Statistical Mechanics and Its Applications* **490**, 819–827 (2018).
  - <sup>45</sup>E. A. Gaiduk, Y. Fomin, E. N. Tsiok, and V. N. Ryzhov, “The influence of random pinning on the melting scenario of two-dimensional soft-disk systems,” *Molecular Physics* **117**, 2910–2919 (2019).
  - <sup>46</sup>Ó. Toledano, M. Pancorbo, J. E. Alvarellos, and Ó. Gálvez, “Melting in two-dimensional systems: Characterizing continuous and first-order transitions,” *Physical Review B* **103**, 094107 (2021).
  - <sup>47</sup>A. Ivlev, H. Löwen, G. Morfill, and C. P. Royall, *Complex plasmas and Colloidal dispersions: particle-resolved studies of classical liquids and solids (Series in soft condensed matter)* (Singapore: World Scientific, 2012).
  - <sup>48</sup>H. Löwen, “Melting, freezing and colloidal suspensions,” *Phys. Rep.* **237**, 249 – 324 (1994).
  - <sup>49</sup>B. Li, D. Zhou, and Y. Han, “Assembly and phase transitions of colloidal crystals,” *Nature Reviews Materials* **1**, 15011 (2016).
  - <sup>50</sup>A. Stradner and P. Schurtenberger, “Potential and limits of a colloidal approach to protein solutions,” *Soft Matter* **16**, 307–323 (2020).
  - <sup>51</sup>A. M. Alsayed, “Premelting at defects within bulk colloidal crystals,” *Science* **309**, 1207–1210 (2005).
  - <sup>52</sup>J. Taffs, S. R. Williams, H. Tanaka, and C. P. Royall, “Structure and kinetics in the freezing of nearly hard spheres,” *Soft Matter* **9**, 297–305 (2013).
  - <sup>53</sup>K. Zahn, R. Lenke, and G. Maret, “Two-stage melting of paramagnetic colloidal crystals in two dimensions,” *Physical Review Letters* **82**, 2721–2724 (1999).
  - <sup>54</sup>K. Zahn and G. Maret, “Dynamic criteria for melting in two dimensions,” *Physical Review Letters* **85**, 3656–3659 (2000).
  - <sup>55</sup>J. Sprakel, A. Zacccone, F. Spaepen, P. Schall, and D. A. Weitz, “Direct observation of entropic stabilization of bcc crystals near melting,” *Physical Review Letters* **118**, 088003 (2017).
  - <sup>56</sup>D. Paloli, P. S. Mohanty, J. J. Crassous, E. Zaccarelli, and P. Schurtenberger, “Fluid-solid transitions in soft-repulsive colloids,” *Soft Matter* **9**, 3000 (2013).
  - <sup>57</sup>Z. Wang, F. Wang, Y. Peng, Z. Zheng, and Y. Han, “Imaging the homogeneous nucleation during the melting of superheated colloidal crystals,” *Science* **338**, 87–90 (2012).
  - <sup>58</sup>E. V. Yakovlev, M. Chaudhuri, N. P. Kryuchkov, P. V. Ovcharov, A. V. Sapelkin, and S. O. Yurchenko, “Experimental validation of interpolation method for pair correlations in model crystals,” *The Journal of Chemical Physics* **151**, 114502 (2019).
  - <sup>59</sup>N. P. Kryuchkov, N. A. Dmitryuk, W. Li, P. V. Ovcharov,

- Y. Han, A. V. Sapelkin, and S. O. Yurchenko, “Mean-field model of melting in superheated crystals based on a single experimentally measurable order parameter,” *Scientific Reports* **11**, 17963 (2021).
- <sup>60</sup>C. P. Royall, M. E. Leunissen, A.-P. Hynninen, M. Dijkstra, and A. van Blaaderen, “Re-entrant melting and freezing in a model system of charged colloids,” *The Journal of Chemical Physics* **124**, 244706 (2006).
- <sup>61</sup>A. Yethiraj and A. van Blaaderen, “A colloidal model system with an interaction tunable from hard sphere to soft and dipolar,” *Nature* **421**, 513–517 (2003).
- <sup>62</sup>Y. Peng, F. Wang, Z. Wang, A. M. Alsayed, Z. Zhang, A. G. Yodh, and Y. Han, “Two-step nucleation mechanism in solid-solid phase transitions,” *Nature Materials* **14**, 101–108 (2014).
- <sup>63</sup>C. P. Royall, D. G. A. L. Aarts, and H. Tanaka, “Bridging length scales in colloidal liquids and interfaces from near-critical divergence to single particles,” *Nature Physics* **3**, 636–640 (2007).
- <sup>64</sup>I. Zhang, C. P. Royall, M. A. Faers, and P. Bartlett, “Phase separation dynamics in colloid–polymer mixtures: the effect of interaction range,” *Soft Matter* **9**, 2076 (2013).
- <sup>65</sup>B. Li, X. Xiao, S. Wang, W. Wen, and Z. Wang, “Real-space mapping of the two-dimensional phase diagrams in attractive colloidal systems,” *Physical Review X* **9** (2019), 10.1103/physrevx.9.031032.
- <sup>66</sup>H. N. Lekkerkerker and R. Tuinier, *Colloids and the Depletion Interaction* (Springer Netherlands, 2011).
- <sup>67</sup>J. E. Martin and A. Snezhko, “Driving self-assembly and emergent dynamics in colloidal suspensions by time-dependent magnetic fields,” *Reports on Progress in Physics* **76**, 126601 (2013).
- <sup>68</sup>J. Byrom and S. L. Biswal, “Magnetic field directed assembly of two-dimensional fractal colloidal aggregates,” *Soft Matter* **9**, 9167 (2013).
- <sup>69</sup>D. Du, D. Li, M. Thakur, and S. L. Biswal, “Generating an in situ tunable interaction potential for probing 2-d colloidal phase behavior,” *Soft Matter* **9**, 6867 (2013).
- <sup>70</sup>Di Du, M. Doxastakis, E. Hilou, and S. L. Biswal, “Two-dimensional melting of colloids with long-range attractive interactions,” *Soft Matter* **13**, 1548–1553 (2017).
- <sup>71</sup>E. Hilou, D. Du, S. Kuei, and S. L. Biswal, “Interfacial energetics of two-dimensional colloidal clusters generated with a tunable anharmonic interaction potential,” *Physical Review Materials* **2**, 025602 (2018).
- <sup>72</sup>D. R. E. Snoswell, C. L. Bower, P. Ivanov, M. J. Cryan, J. G. Rarity, and B. Vincent, “Dynamic control of lattice spacing within colloidal crystals,” *New Journal of Physics* **8**, 267–267 (2006).
- <sup>73</sup>N. Elsner, C. P. Royall, B. Vincent, and D. R. E. Snoswell, “Simple models for two-dimensional tunable colloidal crystals in rotating ac electric fields,” *The Journal of Chemical Physics* **130**, 154901 (2009).
- <sup>74</sup>J. J. Juárez, B. G. Liu, J.-Q. Cui, and M. A. Bevan, “kT-scale colloidal interactions in high-frequency inhomogeneous AC electric fields. II. concentrated ensembles,” *Langmuir* **27**, 9219–9226 (2011).
- <sup>75</sup>T. D. Edwards and M. A. Bevan, “Controlling colloidal particles with electric fields,” *Langmuir* **30**, 10793–10803 (2014).
- <sup>76</sup>J. J. Juárez, S. E. Feicht, and M. A. Bevan, “Electric field mediated assembly of three dimensional equilibrium colloidal crystals,” *Soft Matter* **8**, 94–103 (2012).
- <sup>77</sup>E. V. Yakovlev, K. A. Komarov, K. I. Zaytsev, N. P. Kryuchkov, K. I. Koshelev, A. K. Zotov, D. A. Shelestov, V. L. Tolstoguzov, V. N. Kurllov, A. V. Ivlev, and S. O. Yurchenko, “Tunable two-dimensional assembly of colloidal particles in rotating electric fields,” *Scientific Reports* **7**, 13727 (2017).
- <sup>78</sup>K. A. Komarov, A. V. Yarkov, and S. O. Yurchenko, “Diagrammatic method for tunable interactions in colloidal suspensions in rotating electric or magnetic fields,” *The Journal of Chemical Physics* **151**, 244103 (2019).
- <sup>79</sup>E. V. Yakovlev, N. P. Kryuchkov, S. A. Korsakova, N. A. Dmitryuk, P. V. Ovcharov, M. M. Andronic, I. A. Rodionov, A. V. Sapelkin, and S. O. Yurchenko, “2d colloids in rotating electric fields: A laboratory of strong tunable three-body interactions,” *Journal of Colloid and Interface Science* (2021), 10.1016/j.jcis.2021.09.116.
- <sup>80</sup>K. Müller, N. Osterman, D. Babič, C. N. Likos, J. Dobnikar, and A. Nikoubashman, “Pattern formation and coarse-graining in two-dimensional colloids driven by multiaxial magnetic fields,” *Langmuir* **30**, 5088–5096 (2014).
- <sup>81</sup>N. Osterman, I. Poberaj, J. Dobnikar, D. Frenkel, P. Zihlerl, and D. Babič, “Field-induced self-assembly of suspended colloidal membranes,” *Physical Review Letters* **103**, 228301 (2009).
- <sup>82</sup>A. T. Pham, Y. Zhuang, P. Detwiler, J. E. S. Socolar, P. Charbonneau, and B. B. Yellen, “Phase diagram and aggregation dynamics of a monolayer of paramagnetic colloids,” *Physical Review E* **95**, 052607 (2017).
- <sup>83</sup>K. A. Komarov, N. P. Kryuchkov, and S. O. Yurchenko, “Tunable interactions between particles in conically rotating electric fields,” *Soft Matter* **14**, 9657–9674 (2018).
- <sup>84</sup>K. A. Komarov and S. O. Yurchenko, “Colloids in rotating electric and magnetic fields: designing tunable interactions with spatial field hodographs,” *Soft Matter* **16**, 8155–8168 (2020).
- <sup>85</sup>K. A. Komarov, V. N. Mantsevich, and S. O. Yurchenko, “Core-shell particles in rotating electric and magnetic fields: Designing tunable interactions via particle engineering,” *The Journal of Chemical Physics* **155**, 084903 (2021).
- <sup>86</sup>K. A. Komarov and S. O. Yurchenko, “Diagrammatics of tunable interactions in anisotropic colloids in rotating electric or magnetic fields: New kind of dipole-like interactions,” *The Journal of Chemical Physics* **155**, 114107 (2021).
- <sup>87</sup>P. V. Ovcharov, N. P. Kryuchkov, K. I. Zaytsev, and S. O. Yurchenko, “Particle-resolved phase identification in two-dimensional condensable systems,” *The Journal of Physical Chemistry C* **121**, 26860–26868 (2017).
- <sup>88</sup>E. Luijten and H. W. J. Blöte, “Boundary between long-range and short-range critical behavior in systems with algebraic interactions,” *Physical Review Letters* **89**, 025703 (2002).
- <sup>89</sup>S. S. Khali, D. Chakraborty, and D. Chaudhuri, “Two-step melting of the weeks–chandler–anderson system in two dimensions,” *Soft Matter* **17**, 3473–3485 (2021).

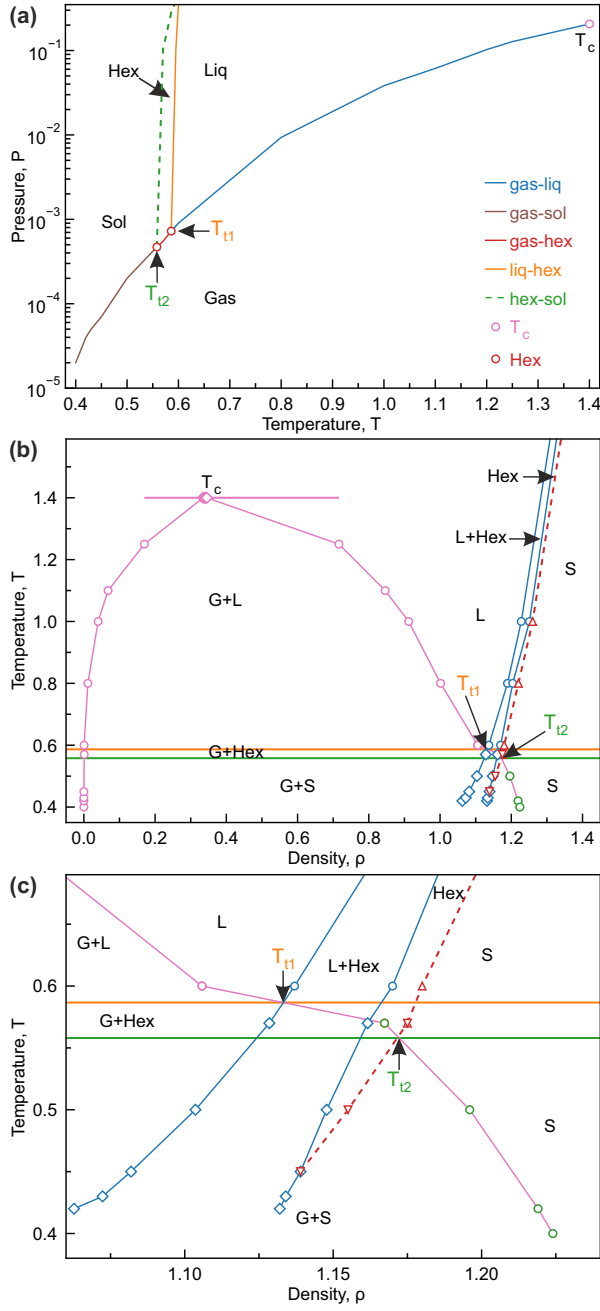


FIG. 11. **The phase diagram of the LJ12-3 system:**

(a) The phase diagram in the  $(P - T)$  coordinates. (b) The phase diagram in the  $(\rho - T)$  coordinates.  $T_{CP}$  is a gas-liquid critical point,  $T_{t1}$  is a hexatic-liquid-gas triple point, and  $T_{t2}$  is a crystal-hexatic-gas triple point. Gas, liquid, hexatic phase and crystal are denoted as G, L, Hex, and S, respectively. The regions of their coexistence are marked as G+L, G+Hex, and G+S. The solid and dashed lines correspond to a first-order transition and to continuous BKT crystal-hexatic phase transition, respectively. The two-stage crystal-gas transition in the metastable area of the hexatic phase and crystal at  $T < T_{t2}$  are denoted with open symbols. (c) The enlarged region of the phase diagram in the area of triple points  $T_{t1}$  and  $T_{t2}$ .